arXiv:1712.01525v3 [hep-ex] 19 Jun 2018

Precision Study of $\eta' \to \gamma\pi^+\pi^-$ Decay Dynamics

M. Ablikim[1], M. N. Achasov[9,e], S. Ahmed[14], X. C. Ai[1], O. Albayrak[5], M. Albrecht[4], D. J. Ambrose[44], A. Amoroso[49A,49C], F. F. An[1], Q. An[46,a], J. Z. Bai[1], R. Baldini Ferroli[20A], Y. Ban[31], D. W. Bennett[19], J. V. Bennett[5], N. Berger[22], M. Bertani[20A], D. Bettoni[21A], J. M. Bian[43], F. Bianchi[49A,49C], E. Boger[23,c], I. Boyko[23], R. A. Briere[5], H. Cai[51], X. Cai[1,a], O. Cakir[40A], A. Calcaterra[20A], G. F. Cao[1], S. A. Cetin[40B], J. Chai[49C], J. F. Chang[1,a], G. Chelkov[23,c,d], G. Chen[1], H. S. Chen[1], J. C. Chen[1], M. L. Chen[1,a], S. Chen[41], S. J. Chen[29], X. Chen[1,a], X. R. Chen[26], Y. B. Chen[1,a], H. P. Cheng[17], X. K. Chu[31], G. Cibinetto[21A], H. L. Dai[1,a], J. P. Dai[34], A. Dbeyssi[14], D. Dedovich[23], Z. Y. Deng[1], A. Denig[22], I. Denysenko[23], M. Destefanis[49A,49C], F. De Mori[49A,49C], Y. Ding[27], C. Dong[30], J. Dong[1,a], L. Y. Dong[1], M. Y. Dong[1,a], Z. L. Dou[29], S. X. Du[53], P. F. Duan[1], J. Z. Fan[39], J. Fang[1,a], S. S. Fang[1], X. Fang[46,a], Y. Fang[1], R. Farinelli[21A,21B], L. Fava[49B,49C], O. Fedorov[23], S. Fegan[22,d], F. Feldbauer[22], G. Felici[20A], C. Q. Feng[46,a], E. Fioravanti[21A], M. Fritsch[14,22], C. D. Fu[1], Q. Gao[1], X. L. Gao[46,a], Y. Gao[39], Z. Gao[46,a], I. Garzia[21A], K. Goetzen[10], L. Gong[30], W. X. Gong[1,a], W. Gradl[22], M. Greco[49A,49C], M. H. Gu[1,a], Y. T. Gu[12], Y. H. Guan[1], A. Q. Guo[1], L. B. Guo[28], R. P. Guo[1], Y. Guo[1], Y. P. Guo[22], Z. Haddadi[25], A. Hafner[22], S. Han[51], X. Q. Hao[15], F. A. Harris[42], K. L. He[1], F. H. Heinsius[4], T. Held[4], Y. K. Heng[1,a], T. Holtmann[4], Z. L. Hou[1], C. Hu[28], H. M. Hu[1], J. F. Hu[49A,49C], T. Hu[1,a], Y. Hu[1], G. S. Huang[46,a], J. S. Huang[15], X. T. Huang[33], X. Z. Huang[29], Y. Huang[29], Z. L. Huang[27], T. Hussain[48], Q. Ji[1], Q. P. Ji[15], X. B. Ji[1], X. L. Ji[1,a], L. W. Jiang[51], X. S. Jiang[1,a], X. Y. Jiang[30], J. B. Jiao[33], Z. Jiao[17], D. P. Jin[1,a], S. Jin[1], T. Johansson[50], A. Julin[43], N. Kalantar-Nayestanaki[25], X. L. Kang[1], X. S. Kang[30], M. Kavatsyuk[25], B. C. Ke[5], P. Kiese[22], R. Kliemt[14], B. Kloss[22], O. B. Kolcu[40B,h], B. Kopf[4], M. Kornicer[42], A. Kupsc[50], W. Kühn[24], J. S. Lange[24], M. Lara[19], P. Larin[14], H. Leithoff[22], C. Leng[49C], C. Li[50], Cheng Li[46,a], D. M. Li[53], F. Li[1,a], F. Y. Li[31], G. Li[1], H. B. Li[1], H. J. Li[1], J. C. Li[1], Jin Li[32], K. Li[13], K. Li[33], Lei Li[3], P. R. Li[41], Q. Y. Li[33], T. Li[33], W. D. Li[1], W. G. Li[1], X. L. Li[33], X. N. Li[1,a], X. Q. Li[30], Y. B. Li[2], Z. B. Li[38], H. Liang[46,a], Y. F. Liang[36], Y. T. Liang[24], G. R. Liao[11], D. X. Lin[14], B. Liu[34], B. J. Liu[1], C. X. Liu[1], D. Liu[46,a], F. H. Liu[35], Fang Liu[1], Feng Liu[6], H. B. Liu[12], H. H. Liu[16], H. H. Liu[1], H. M. Liu[1], J. Liu[1], J. B. Liu[46,a], J. P. Liu[51], J. Y. Liu[1], K. Liu[39], K. Y. Liu[27], L. D. Liu[31], P. L. Liu[1,a], Q. Liu[41], S. B. Liu[46,a], X. Liu[26], Y. B. Liu[30], Y. Y. Liu[30], Z. A. Liu[1,a], Zhiqing Liu[22], H. Loehner[25], Y. F. Long[31], X. C. Lou[1,a,g], H. J. Lu[17], J. G. Lu[1,a], Y. Lu[1], Y. P. Lu[1,a], C. L. Luo[28], M. X. Luo[52], T. Luo[42], X. L. Luo[1,a], X. R. Lyu[41], F. C. Ma[27], H. L. Ma[1], L. L. Ma[33], M. M. Ma[1], Q. M. Ma[1], T. Ma[1], X. N. Ma[30], X. Y. Ma[1,a], Y. M. Ma[33], F. E. Maas[14], M. Maggiora[49A,49C], Q. A. Malik[48], Y. J. Mao[31], Z. P. Mao[1], S. Marcello[49A,49C], J. G. Messchendorp[25], G. Mezzadri[21B], J. Min[1,a], T. J. Min[1], R. E. Mitchell[19], X. H. Mo[1,a], Y. J. Mo[6], C. Morales Morales[14], N. Yu. Muchnoi[9,e], H. Muramatsu[43], P. Musiol[4], Y. Nefedov[23], F. Nerling[14], I. B. Nikolaev[9,e], Z. Ning[1,a], S. Nisar[8], S. L. Niu[1,a], X. Y. Niu[1], S. L. Olsen[32], Q. Ouyang[1,a], S. Pacetti[20B], Y. Pan[46,a], P. Patteri[20A], M. Pelizaeus[4], H. P. Peng[46,a], K. Peters[10,i], J. Pettersson[50], J. L. Ping[28], R. G. Ping[1], R. Poling[43], V. Prasad[1], H. R. Qi[2], M. Qi[29], S. Qian[1,a], C. F. Qiao[41], L. Q. Qin[33,1], N. Qin[51], X. S. Qin[1], Z. H. Qin[1,a], J. F. Qiu[1], K. H. Rashid[48], C. F. Redmer[22], M. Ripka[22], G. Rong[1], Ch. Rosner[14], X. D. Ruan[12], A. Sarantsev[23,f], M. Savrié[21B], C. Schnier[4], K. Schoenning[50], S. Schumann[22], W. Shan[31], M. Shao[46,a], C. P. Shen[2], P. X. Shen[30], X. Y. Shen[1], H. Y. Sheng[1], M. Shi[1], W. M. Song[1], X. Y. Song[1], S. Sosio[49A,49C], S. Spataro[49A,49C], G. X. Sun[1], J. F. Sun[15], S. S. Sun[1], X. H. Sun[1], Y. J. Sun[46,a], Y. Z. Sun[1], Z. J. Sun[1,a], Z. T. Sun[19], C. J. Tang[36], X. Tang[1], I. Tapan[40C], E. H. Thorndike[44], M. Tiemens[25], I. Uman[40D], G. S. Varner[42], B. Wang[30], B. L. Wang[41], D. Wang[31], D. Y. Wang[31], K. Wang[1,a], L. L. Wang[1], L. S. Wang[1], M. Wang[33], P. Wang[1], P. L. Wang[1], W. Wang[1,a], W. P. Wang[46,a], X. F. Wang[39], Y. Wang[37], Y. D. Wang[14], Y. F. Wang[1,a], Y. Q. Wang[22], Z. Wang[1,a], Z. G. Wang[1,a], Z. H. Wang[46,a], Z. Y. Wang[1], Z. Y. Wang[1], T. Weber[22], D. H. Wei[11], P. Weidenkaff[22], S. P. Wen[1], U. Wiedner[4], M. Wolke[50], L. H. Wu[1], L. J. Wu[1], Z. Wu[1,a], L. Xia[46,a], L. G. Xia[39], Y. Xia[18], D. Xiao[1], H. Xiao[47], Z. J. Xiao[28], Y. G. Xie[1,a], Q. L. Xiu[1,a], G. F. Xu[1], J. J. Xu[1], L. Xu[1], Q. J. Xu[13], Q. N. Xu[41], X. P. Xu[37], L. Yan[49A,49C], W. B. Yan[46,a], W. C. Yan[46,a], Y. H. Yan[18], H. J. Yang[34,j], H. X. Yang[1], L. Yang[51], Y. X. Yang[11], M. Ye[1,a], M. H. Ye[7], J. H. Yin[1], Z. Y. You[38], B. X. Yu[1,a], C. X. Yu[30], J. S. Yu[26], C. Z. Yuan[1], W. L. Yuan[29], Y. Yuan[1], A. Yuncu[40B,b], A. A. Zafar[48], A. Zallo[20A], Y. Zeng[18], Z. Zeng[46,a], B. X. Zhang[1], B. Y. Zhang[1,a], C. Zhang[29], C. C. Zhang[1], D. H. Zhang[1], H. H. Zhang[38], H. Y. Zhang[1,a], J. Zhang[1], J. J. Zhang[1], J. L. Zhang[1], J. Q. Zhang[1], J. W. Zhang[1,a], J. Y. Zhang[1], J. Z. Zhang[1], K. Zhang[1], L. Zhang[1], S. Q. Zhang[30], X. Y. Zhang[33], Y. Zhang[1], Y. Zhang[1], Y. H. Zhang[1,a], Y. N. Zhang[41], Y. T. Zhang[46,a], Yu Zhang[41], Z. H. Zhang[6], Z. P. Zhang[46], Z. Y. Zhang[51], G. Zhao[1], J. W. Zhao[1,a], J. Y. Zhao[1], J. Z. Zhao[1,a], Lei Zhao[46,a], Ling Zhao[1], M. G. Zhao[30], Q. Zhao[1], Q. W. Zhao[1], S. J. Zhao[53], T. C. Zhao[1], Y. B. Zhao[1,a], Z. G. Zhao[46,a], A. Zhemchugov[23,c], B. Zheng[47], J. P. Zheng[1,a], W. J. Zheng[33], Y. H. Zheng[41], B. Zhong[28], L. Zhou[1,a], X. Zhou[51], X. K. Zhou[46,a], X. R. Zhou[46,a], X. Y. Zhou[1], K. Zhu[1], K. J. Zhu[1,a], S. Zhu[1], S. H. Zhu[45], X. L. Zhu[39], Y. C. Zhu[46,a], Y. S. Zhu[1], Z. A. Zhu[1], J. Zhuang[1,a], L. Zotti[49A,49C], B. S. Zou[1], J. H. Zou[1]

(BESIII Collaboration)

[1] *Institute of High Energy Physics, Beijing 100049, People's Republic of China*
[2] *Beihang University, Beijing 100191, People's Republic of China*
[3] *Beijing Institute of Petrochemical Technology, Beijing 102617, People's Republic of China*
[4] *Bochum Ruhr-University, D-44780 Bochum, Germany*
[5] *Carnegie Mellon University, Pittsburgh, Pennsylvania 15213, USA*
[6] *Central China Normal University, Wuhan 430079, People's Republic of China*
[7] *China Center of Advanced Science and Technology, Beijing 100190, People's Republic of China*
[8] *COMSATS Institute of Information Technology, Lahore, Defence Road, Off Raiwind Road, 54000 Lahore, Pakistan*
[9] *G.I. Budker Institute of Nuclear Physics SB RAS (BINP), Novosibirsk 630090, Russia*
[10] *GSI Helmholtzcentre for Heavy Ion Research GmbH, D-64291 Darmstadt, Germany*
[11] *Guangxi Normal University, Guilin 541004, People's Republic of China*

[12] Guangxi University, Nanning 530004, People's Republic of China
[13] Hangzhou Normal University, Hangzhou 310036, People's Republic of China
[14] Helmholtz Institute Mainz, Johann-Joachim-Becher-Weg 45, D-55099 Mainz, Germany
[15] Henan Normal University, Xinxiang 453007, People's Republic of China
[16] Henan University of Science and Technology, Luoyang 471003, People's Republic of China
[17] Huangshan College, Huangshan 245000, People's Republic of China
[18] Hunan University, Changsha 410082, People's Republic of China
[19] Indiana University, Bloomington, Indiana 47405, USA
[20] (A)INFN Laboratori Nazionali di Frascati, I-00044, Frascati, Italy; (B)INFN and University of Perugia, I-06100, Perugia, Italy
[21] (A)INFN Sezione di Ferrara, I-44122, Ferrara, Italy; (B)University of Ferrara, I-44122, Ferrara, Italy
[22] Johannes Gutenberg University of Mainz, Johann-Joachim-Becher-Weg 45, D-55099 Mainz, Germany
[23] Joint Institute for Nuclear Research, 141980 Dubna, Moscow region, Russia
[24] Justus-Liebig-Universitaet Giessen, II. Physikalisches Institut, Heinrich-Buff-Ring 16, D-35392 Giessen, Germany
[25] KVI-CART, University of Groningen, NL-9747 AA Groningen, The Netherlands
[26] Lanzhou University, Lanzhou 730000, People's Republic of China
[27] Liaoning University, Shenyang 110036, People's Republic of China
[28] Nanjing Normal University, Nanjing 210023, People's Republic of China
[29] Nanjing University, Nanjing 210093, People's Republic of China
[30] Nankai University, Tianjin 300071, People's Republic of China
[31] Peking University, Beijing 100871, People's Republic of China
[32] Seoul National University, Seoul, 151-747 Korea
[33] Shandong University, Jinan 250100, People's Republic of China
[34] Shanghai Jiao Tong University, Shanghai 200240, People's Republic of China
[35] Shanxi University, Taiyuan 030006, People's Republic of China
[36] Sichuan University, Chengdu 610064, People's Republic of China
[37] Soochow University, Suzhou 215006, People's Republic of China
[38] Sun Yat-Sen University, Guangzhou 510275, People's Republic of China
[39] Tsinghua University, Beijing 100084, People's Republic of China
[40] (A)Ankara University, 06100 Tandogan, Ankara, Turkey; (B)Istanbul Bilgi University, 34060 Eyup, Istanbul, Turkey; (C)Uludag University, 16059 Bursa, Turkey; (D)Near East University, Nicosia, North Cyprus, Mersin 10, Turkey
[41] University of Chinese Academy of Sciences, Beijing 100049, People's Republic of China
[42] University of Hawaii, Honolulu, Hawaii 96822, USA
[43] University of Minnesota, Minneapolis, Minnesota 55455, USA
[44] University of Rochester, Rochester, New York 14627, USA
[45] University of Science and Technology Liaoning, Anshan 114051, People's Republic of China
[46] University of Science and Technology of China, Hefei 230026, People's Republic of China
[47] University of South China, Hengyang 421001, People's Republic of China
[48] University of the Punjab, Lahore-54590, Pakistan
[49] (A)University of Turin, I-10125, Turin, Italy; (B)University of Eastern Piedmont, I-15121, Alessandria, Italy; (C)INFN, I-10125, Turin, Italy
[50] Uppsala University, Box 516, SE-75120 Uppsala, Sweden
[51] Wuhan University, Wuhan 430072, People's Republic of China
[52] Zhejiang University, Hangzhou 310027, People's Republic of China
[53] Zhengzhou University, Zhengzhou 450001, People's Republic of China
[a] Also at State Key Laboratory of Particle Detection and Electronics, Beijing 100049, Hefei 230026, People's Republic of China
[b] Also at Bogazici University, 34342 Istanbul, Turkey
[c] Also at the Moscow Institute of Physics and Technology, Moscow 141700, Russia
[d] Also at the Functional Electronics Laboratory, Tomsk State University, Tomsk, 634050, Russia
[e] Also at the Novosibirsk State University, Novosibirsk, 630090, Russia
[f] Also at the NRC "Kurchatov Institute", PNPI, 188300, Gatchina, Russia
[g] Also at University of Texas at Dallas, Richardson, Texas 75083, USA
[h] Also at Istanbul Arel University, 34295 Istanbul, Turkey
[i] Also at Goethe University Frankfurt, 60323 Frankfurt am Main, Germany
[j] Also at Institute of Nuclear and Particle Physics, Shanghai Key Laboratory for Particle Physics and Cosmology, Shanghai 200240, People's Republic of China

Using a low background data sample of 9.7×10^5 $J/\psi \to \gamma\eta'$, $\eta' \to \gamma\pi^+\pi^-$ events, which are 2 orders of magnitude larger than those from the previous experiments, recorded with the BESIII detector at BEPCII, the decay dynamics of $\eta' \to \gamma\pi^+\pi^-$ are studied with both model-dependent and model-independent approaches. The contributions of ω and the $\rho(770) - \omega$ interference are observed for the first time in the decays $\eta' \to \gamma\pi^+\pi^-$ in both approaches. Additionally, a contribution from the box anomaly or the $\rho(1450)$ resonance is required in the model-dependent approach, while the

process specific part of the decay amplitude is determined in the model-independent approach.

PACS numbers: 13.20.Gd, 14.40.Be

The radiative decay $\eta' \to \gamma\pi^+\pi^-$ is the second most probable decay mode of the η' meson with a branching fraction of $(28.9 \pm 0.5)\%$ [1] and is frequently used for tagging η' candidates. In the vector meson dominance (VMD) model [2], this process is dominated by the decay $\eta' \to \gamma\rho(770)$ (hereafter referred to as ρ^0). In the past, the dipion mass distribution was studied by several experiments, *e.g.*, JADE [3], CELLO [4], PLUTO [5], TASSO [6], TPC/$\gamma\gamma$ [7], and ARGUS [8], and a peak shift of about +20 MeV/c^2 for the ρ^0 meson with respect to the expected position was observed. Dedicated studies, using about 2000 $\eta' \to \gamma\pi^+\pi^-$ events, concluded that a lone ρ^0 contribution in the dipion mass spectrum did not describe the experimental data [9]. This discrepancy could be attributed to a higher term of the Wess-Zumino-Witten anomaly, known as the box anomaly, in the chiral perturbation theory (ChPT) Lagrangian [10]. To determine the ratio of these two contributions, it was suggested to fit the dipion invariant mass spectrum by including an extra nonresonant term in the decay amplitude to account for the box anomaly contribution [11]. Using a sample of 7490±180 η' events, evidence for the box anomaly contribution with a 4σ significance was reported by the Crystal Barrel experiment [12], whereas the observation was not confirmed by the L3 experiment [13] using 2123±53 events.

A recently proposed model-independent approach [14], based on ChPT and dispersion theory, relates the $\eta/\eta' \to \gamma\pi^+\pi^-$ decay amplitudes directly to the $e^+e^- \to \pi^+\pi^-$ process, which dominates the hadron production cross section at low energies and gives the largest hadronic contribution to the muon anomalous magnetic moment [15]. The amplitudes for $\eta/\eta' \to \gamma\pi^+\pi^-$ therein are given as a product of the pion vector form factor $F_V(s)$ and a reaction specific part $P(s)$, where s is the $\pi^+\pi^-$ invariant mass squared. The $F_V(s)$ term is extracted from the $e^+e^- \to \pi^+\pi^-$ cross section or from P-wave isovector $\pi\pi$ phase shifts. The $P(s)$ term, which can be expanded into a Taylor series around $s = 0$, is expected to be similar for η and η' decays [16], and has been determined in η decays by WASA-at-COSY [17] and KLOE [18], but not yet for η' decays due to the limited statistics.

In this Letter, we present a precision measurement of the dipion mass distribution for the $\eta' \to \gamma\pi^+\pi^-$ process originating from the radiative decays $J/\psi \to \gamma\eta'$ based on $(1310.6 \pm 7.0) \times 10^6$ J/ψ events [19], which is produced in e^+e^- annihilation, collected with the BESIII detector [20]. Both model-dependent and model-independent approaches are used to investigate the decay dynamics.

Candidates of $J/\psi \to \gamma\eta'$, $\eta' \to \gamma\pi^+\pi^-$ are required to have two charged tracks with opposite charge and at least two photons. The selection criteria for charged tracks and photon candidates are the same as those in Ref. [21], except for the minimum energy requirement of the photon candidates on the barrel showers, which is 40 MeV instead of 25 MeV in this analysis.

A four-constraint (4C) energy-momentum conservation kinematic fit is performed under the $\gamma\gamma\pi^+\pi^-$ hypothesis, and a loose requirement of $\chi^2_{4C} < 100$ is imposed. This requirement removes 39.3% background while the efficiency loss is 2.1%. For events with more than two photon candidates, the combination with the smallest χ^2_{4C} is retained. In order to remove background events with a π^0 in the final states (*e.g.*, $J/\psi \to \pi^+\pi^-\pi^0, \gamma\pi^+\pi^-\pi^0$), we require that the $\gamma\gamma$ invariant mass is outside the π^0 mass region, $|M(\gamma\gamma) - m_{\pi^0}| > 0.02$ GeV/c^2, where m_{π^0} is the nominal mass of the π^0 [1]. Since the radiative photon from the η' is always more soft than that from the J/ψ decays, the $\gamma\pi^+\pi^-$ combinations closest to the nominal η' mass ($m_{\eta'}$), are kept as η' candidates. After the above selection, a clear η' signal is observed in the $\gamma\pi^+\pi^-$ invariant mass spectrum, as shown in Fig. 1. To select candidate events from η' decays, $|M(\gamma\pi^+\pi^-) - m_{\eta'}| < 0.02$ GeV/c^2 is required.

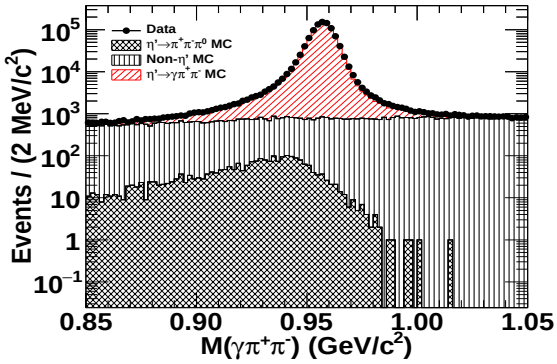


FIG. 1. Invariant mass spectrum of $\gamma\pi^+\pi^-$. Dots with error bars represent the data, and the hatched histograms are MC simulations, where the backgrounds are normalized to the expected contributions as described in the text.

An inclusive Monte Carlo (MC) sample of 1.2×10^9 J/ψ decay events that are generated with the LUNDCHARM and EVTGEN models [22, 23] is used to investigate possible background processes. These include events with no η''s in the final state (non-η') and those from $\eta' \to \pi^+\pi^-\pi^0$. We use the events in the η' mass sideband regions ($0.04 < |M(\gamma\pi^+\pi^-) - m_{\eta'}| < 0.06$ GeV/c^2) to estimate the non-η' background contribution, which is at a level of 1.42%. For the $\eta' \to \pi^+\pi^-\pi^0(\gamma\gamma)$ back-

ground, a MC study predicts the number of background events to be 0.16%, and its effect is not included in the fit, but taken into consideration in the systematic uncertainty study.

With the η' mass window requirement, a low background sample of about 9.7×10^5 η' candidates is obtained, which is about 120 times larger than the previous largest sample reported by the Crystal Barrel experiment [12]. The background subtracted and efficiency corrected angular distribution of π^+ in the helicity frame of the $\pi^+\pi^-$ system, $|\cos\theta_{\pi^+}|$, is shown in Fig. 2. The distribution is very well described by $dN/d\cos\theta_{\pi^+} \propto \sin^2\theta_{\pi^+}$, which is expected for a P-wave dipion system. A detailed MC study indicates that the reconstructed $\pi^+\pi^-$ invariant mass $M(\pi^+\pi^-)$ has a small shift with respect to the true value, and this is corrected as a function of $M(\pi^+\pi^-)$ according to the values obtained in MC studies. The maximum shift is less than 0.75 MeV/c^2. The $M(\pi^+\pi^-)$ distribution with the mass shift correction is illustrated as dots with error bars in Fig. 3.

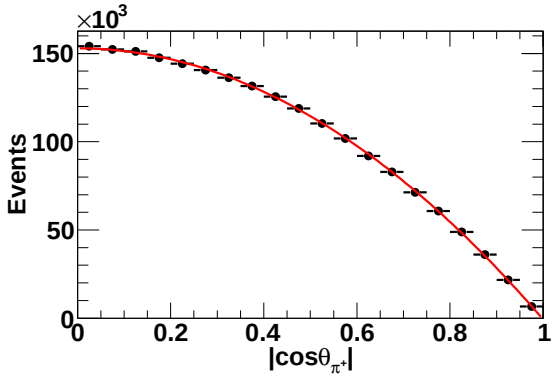


FIG. 2. Background subtracted and efficiency corrected angular distribution of π^+ in the helicity frame of the $\pi^+\pi^-$ system. Dots with error bars are data, and the curve is the fit with a $\sin^2\theta_{\pi^+}$ function.

The dipion mass dependent differential rate is given by [12] $\frac{d\Gamma}{dM(\pi^+\pi^-)} = \frac{k_\gamma^3 q_\pi^3(s)}{48\pi^3}|\mathcal{A}|^2$, where $k_\gamma = (m_{\eta'}^2 - s)/(2m_{\eta'})$, $q_\pi(s) = \sqrt{s - 4m_\pi^2}/2$ and $\mathcal{A}$ is the decay amplitude. Both the model-dependent and model-independent approaches are carried out to investigate the decay dynamics.

In the model-dependent study, by assuming that the possible non-ρ^0 contributions are from ω, $\rho(1450)$ (hereafter referred to as ρ'), and the box anomaly, we have [11, 12, 24]

$$\mathcal{A} = \frac{BW_\rho^{GS}(s)(1+\delta\frac{s}{M_\omega^2}BW_\omega(s)) + \beta BW_{\rho'}^{GS}(s)}{1+\beta} \times 2\sqrt{48\pi M_\rho^{-4}} + \alpha,$$

where δ and β are complex numbers representing the contributions of the ω and ρ' mesons relative to the ρ^0; α is a constant accounting for the box anomaly contribution [11]; and $BW_\rho^{GS}(s)$, $BW_\omega(s)$, and $BW_{\rho'}^{GS}(s)$ are the propagators for the ρ^0, ω, and ρ' mesons, respectively. Since the ρ^0 component is dominant in the $M(\pi^+\pi^-)$ distribution, its shape parametrization plays a vital role in the determination of other components, and is represented with the Gounaris-Sakurai approach (GS) [25, 26]. $BW_\omega(s) = M_\omega^2/(M_\omega^2 - s - iM_\omega\Gamma_\omega)$, where M_ω and Γ_ω are the ω-meson mass and width, respectively. The ρ' is also described with the GS parametrization. The masses and widths for the ω and ρ' mesons are fixed to their nominal values [1], while those for ρ^0 are floated in the fit.

Binned maximum likelihood fits are performed to the $M(\pi^+\pi^-)$ distribution between 0.34 and 0.90 GeV/c^2 with different scenarios, where the decay amplitude is corrected by a $M(\pi^+\pi^-)$-dependent detection efficiency and is smeared with a $M(\pi^+\pi^-)$-dependent Gaussian function to account for the experimental mass resolution. The non-η' background is represented by the η' sideband events as discussed above, and is fixed in the fit. Fits with only the ρ^0 contribution and with additional ρ^0-ω interference give the goodness of fit χ^2/ndf=3365/110 and 3094/108, respectively, where ndf is the number of degrees of freedom. The results indicate that these components are insufficient to describe the data and extra contributions are necessary. To improve the description of the data, we performed a fit, shown in Fig. 3(a), including the additional box anomaly term together with ρ^0-ω interference, and much better agreement with χ^2/ndf=207/107 is obtained. An alternative fit by replacing the box anomaly with the ρ' component gives considerably worse agreement with χ^2/ndf=303/106, as illustrated in Fig. 3(b). Fit results of the above two cases are summarized in Table I. Both cases yield ρ^0 mass and width close to those in the PDG [1]. A fit including both the ρ' and box anomaly gives a reasonable goodness of fit (χ^2/ndf =134/105). However, a very strong correlation in amplitude between the box anomaly and the ρ' components, *i.e.* the correlation coefficient is -0.986, is observed, due to the tail of the ρ' having a similar line shape as that of the box anomaly. Thus they are not well under control, and it is hard for one to distinguish them in the fitting. Whereas the mass and width of the ρ^0 are stable, which are 776.43 ± 0.36, 150.26 ± 0.56 MeV/c^2, respectively. Therefore a refined model dependent amplitude beyond including just the ρ' or the box anomaly contribution is desirable.

As suggested by Ref. [14], a model independent approach is also implemented to investigate the decay dynamics. The decay amplitude follows $\mathcal{A} = NP(s)F_V(s)$, where N is a normalization factor, a polynomial function $P(s) = 1+\kappa s+\lambda s^2+\xi BW_\omega+\mathcal{O}(s^4)$ includes the possible ω term ξ and quadratic term λ, and the pion vector form factor $F_V(s)$ is obtained from $e^+e^- \to \pi^+\pi^-$ measure-

TABLE I. The results of the model-dependent fits to the $M(\pi^+\pi^-)$ distribution in different cases. The first uncertainties are statistical and the second ones systematic.

Model-dependent fit	ρ^0-ω-box anomaly	ρ^0-ω-ρ'
$M(\rho^0)$ [MeV/c^2]	774.34 ± 0.18 ± 0.35	772.93 ± 0.18 ± 0.34
$\Gamma(\rho^0)$ [MeV]	150.85 ± 0.55 ± 0.67	150.18 ± 0.55 ± 0.65
arg δ [rad]	(0.65 ± 3.14 ± 2.62)×10^{-2}	(-2.59 ± 3.19 ± 2.62)×10^{-2}
$\lvert\delta\rvert$ [10^{-3}]	1.61 ± 0.05 ± 0.13	1.59 ± 0.05 ± 0.11
arg β [rad]	...	3.28 ± 0.11 ± 0.04
$\lvert\beta\rvert$	...	0.26 ± 0.01 ± 0.01
α [MeV^{-2}]	-11.56 ± 0.21 ± 0.32	...
$\mathcal{B}(\eta' \to \gamma\rho^0)$	(33.34 ± 0.06 ± 1.60)%	(34.43 ± 0.52 ± 1.97)%
$\mathcal{B}(\eta' \to \gamma\omega \to \gamma\pi^+\pi^-)$	(3.25 ± 0.21 ± 0.52)×10^{-4}	(3.22 ± 0.21 ± 0.52)×10^{-4}
$\mathcal{B}(\eta' \to \gamma\pi^+\pi^-$ via box)	(2.45 ± 0.09 ± 0.19)×10^{-3}	...
$\mathcal{B}(\eta' \to \gamma\pi^+\pi^-$ via ρ')	...	(3.43 ± 0.38 ± 0.28)×10^{-3}

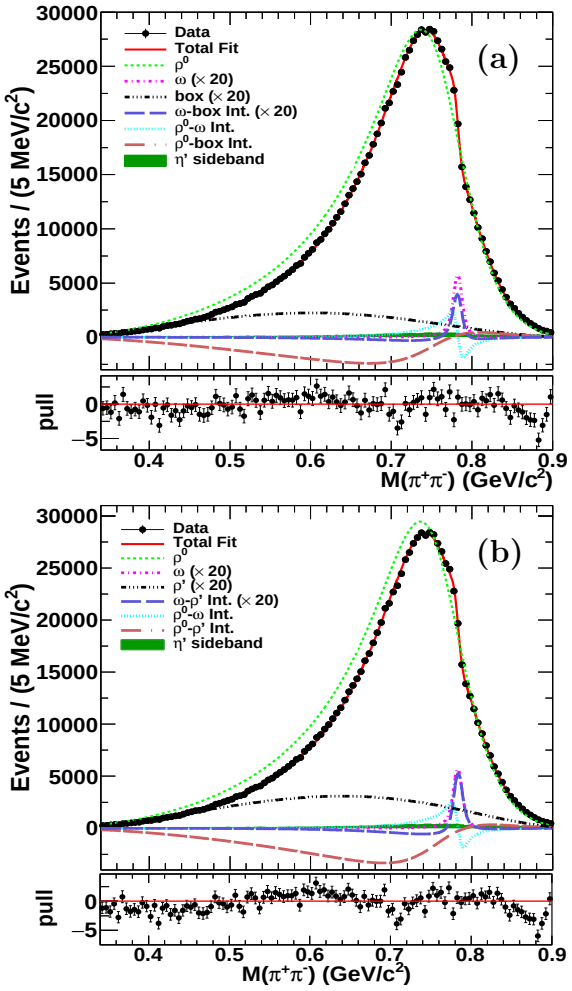


FIG. 3. Model-dependent fit results in case (a) ρ^0-ω-box anomaly and (b) ρ^0-ω-ρ'. Dots with error bars represent data, the green shaded histograms are the background from η' sideband events, the red solid curves are the total fit results, and others represent the separate contributions as indicated. To be visible, the small contributions of ω, the box anomaly (ρ') and the interference between ω and the box anomaly (ρ') are scaled by a factor of 20.

ments [27–31].

A fit to the data gives $\kappa = 0.992 \pm 0.039$ GeV^{-2}, $\lambda = -0.523 \pm 0.039$ GeV^{-4}, $\xi = 0.199 \pm 0.006$ with χ^2/ndf=145/109, where the uncertainties are statistical only. The fit result is shown in Fig. 4, and the statistical significances of nonzero quadratic term and ω term are 13σ and 34σ, respectively, which are estimated with the changes of the log likelihood value and the number of degree of freedoms. An alternative fit without the ω contribution yields $\kappa = 1.420 \pm 0.047$ GeV^{-2} and $\lambda = -0.951 \pm 0.046$ GeV^{-4}, which is compatible to a recent prediction $\lambda = -1.0 \pm 0.1$ GeV^{-4} [32]. However, this fit corresponds to a very poor goodness of fit (χ^2/ndf =1351/110) and fails to describe the data. Different from the measurements of $\eta \to \gamma\pi^+\pi^-$ decays [17, 18], which are not sensitive to the quadratic term, both the quadratic term and the ω contribution are significant in the $\eta' \to \gamma\pi^+\pi^-$ decays.

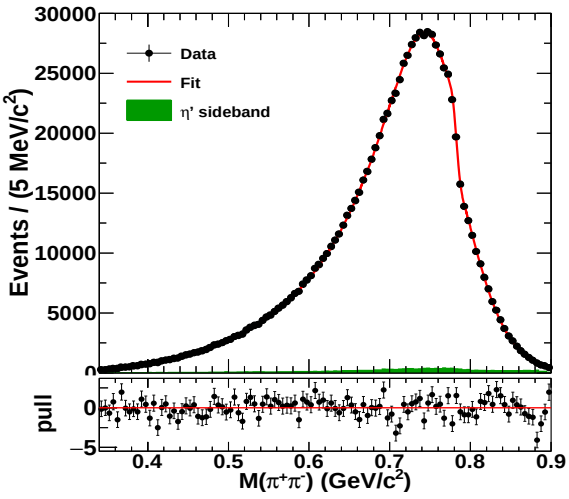


FIG. 4. The results of the model-independent fit with ω interference. Dots with error bars represent data, the (green) shaded histogram is the background contribution from η' sideband events, and the (red) solid curve is the fit result.

The systematic uncertainties in the model-dependent and model-independent approaches are discussed in detail in the following and are summarized in the Supplemental Material [33]. The total systematic uncertainty is the quadrature sum of the individual values by assuming them to be independent.

The uncertainty associated with the 4C kinematic fit originates from the difference between data and MC simulation. This difference is reduced by correcting the track helix parameters of the MC sample as described in Ref. [34]. To estimate the corresponding uncertainty, the analysis is repeated without the track helix parameters correction, and the resultant change is assigned as the uncertainty.

The MDC tracking and photon detection efficiencies are studied based on a clean sample of $J/\psi \to \rho\pi$. The differences between data and MC simulation are investigated as a function of momentum (energy), and are less than 1% for each charged track and 1% for each photon [35]. To evaluate their impact on the results, an event-by-event correction on the tracking and photon detection efficiency is performed as a function of momentum (energy). The resultant changes on the results are taken as the systematic uncertainties.

The uncertainty from the η' mass window requirement is evaluated by varying the required values by $\pm$ 6 MeV/c^2, which is the mass resolution from the MC simulation, and the maximum change of the results is taken as the uncertainty.

Systematic sources related with the fit procedure include the binning, the fit range, the background, the mass resolution of $M(\pi^+\pi^-)$, and the input parameters in the fit. The uncertainty from binning is studied with the same fit procedure with varied bin width. For the uncertainty due to the fit range, we take the larger change of the fit result with varied fit ranges as the uncertainty. Two systematic sources, *i.e.* the η' sideband and the small contribution of $\eta' \to \pi^+\pi^-\pi^0$, are considered as the uncertainty related with the background in the fit. The former one is estimated by changing the sideband region, while the latter one is studied by including the background in the fit with a fixed magnitude and shape in accordance with the MC study. We assign the quadratic sum of the two uncertainties as the total background uncertainty. The impact caused by the $\pi^+\pi^-$ mass resolution is estimated by varying the resolution by $\pm$10% in the fit, and the maximum change of the fit result is assigned as the uncertainty. For the model dependent study, the uncertainty due to the mass and width of ω, ρ' resonances is estimated by varying the input values with $\pm1\sigma$ of the corresponding uncertainties from the PDG [1], respectively, and taking the quadratic sum of the maximum change of the fit results as the uncertainty of the resonance parameters.

For the measurement of the branching fraction of η' decays into $\gamma\rho^0$, $\gamma\omega$, γ box anomaly and $\gamma\rho'$, the additional uncertainties from the branching fractions of $J/\psi \to \gamma\eta'$ [1] and the number of J/ψ events [19] are also taken into account.

In the model independent approach, the uncertainty associated with the input pion vector form factor $F_V(s)$, is estimated by an alternative fit incorporating the line shape of $F_V(s)$ from Ref. [36]. The resulting differences, 16.4%, 34.7%, and 3.4% for the κ, λ, ξ parameters, respectively, determine the systematic uncertainty. Since this uncertainty is theoretically dependent, it is treated as a separated uncertainty in the final results.

In summary, the $\eta' \to \gamma\pi^+\pi^-$ decay dynamics is studied based on a sample of 9.7×10^5 events originating from the radiative decay $J/\psi \to \gamma\eta'$ of 1.31×10^9 J/ψ events collected with the BESIII detector. We have measured the dipion invariant mass distribution and performed fits using model dependent and independent approaches. For the first time, the ω contribution is observed in the dipion mass spectrum in the decays $\eta' \to \gamma\pi^+\pi^-$. The model-dependent fit indicates that only the components of ρ^0 and ω as well as the corresponding interference fail to describe the data, and an extra significant contribution, *i.e.* the box anomaly or ρ', is found to be necessary for the first time. The corresponding fit results and the measured branching fractions are summarized in Table I. The data call for a more complete model-dependent amplitude beyond just including the box anomaly or ρ' contribution for the $M(\pi^+\pi^-)$ spectrum.

The model independent approach [14] provides a satisfactory parametrization of the dipion invariant mass spectrum, and yields the parameters of the process-specific part $P(s)$ to be $\kappa = 0.992 \pm 0.039 \pm 0.067 \pm 0.163$ GeV^{-2}, $\lambda = -0.523 \pm 0.039 \pm 0.066 \pm 0.181$ GeV^{-4}, and $\xi = 0.199 \pm 0.006 \pm 0.011 \pm 0.007$, where the first uncertainties are statistical, the second are systematic, and the third are theoretical. In contrast to the conclusion in Ref. [14] based on the limited statistics from the Crystal Barrel experiment [12], our result indicates that the quadratic term and the ω contribution in $P(s)$, corresponding to statistical significances of 13σ and 34σ, respectively, are necessary.

The BESIII Collaboration thanks the staff of BEPCII and the IHEP computing center for their strong support. This work is supported in part by National Key Basic Research Program of China under Contract No. 2015CB856700; National Natural Science Foundation of China (NSFC) under Contracts No. 11565006, No. 11235011, No. 11335008, No. 11425524, No. 11625523, No. 11635010, No. 11675184, No. 11735014; the Chinese Academy of Sciences (CAS) Large-Scale Scientific Facility Program; the CAS Center for Excellence in Particle Physics (CCEPP); Joint Large-Scale Scientific Facility Funds of the NSFC and CAS under Contracts No. U1332201, No. U1532257, No. U1532258; CAS Key Research Program of Frontier Sciences under Contracts No. QYZDJ-SSW-SLH003, No. QYZDJ-

SSW-SLH040; 100 Talents Program of CAS; National 1000 Talents Program of China; Shandong Natural Science Funds for Distinguished Young Scholar under Contract No. JQ201402; INPAC and Shanghai Key Laboratory for Particle Physics and Cosmology; German Research Foundation DFG under Contracts Nos. Collaborative Research Center CRC 1044, FOR 2359; Istituto Nazionale di Fisica Nucleare, Italy; Koninklijke Nederlandse Akademie van Wetenschappen (KNAW) under Contract No. 530-4CDP03; Ministry of Development of Turkey under Contract No. DPT2006K-120470; National Natural Science Foundation of China (NSFC) under Contracts No. 11505034, No. 11575077; National Science and Technology fund; The Swedish Research Council; U. S. Department of Energy under Contracts No. DE-FG02-05ER41374, No. DE-SC-0010118, No. DE-SC-0010504, No. DE-SC-0012069; University of Groningen (RuG) and the Helmholtzzentrum fuer Schwerionenforschung GmbH (GSI), Darmstadt; WCU Program of National Research Foundation of Korea under Contract No. R32-2008-000-10155-0.

[1] C. Patrignani *et al.* (Particle Data Group), Chin. Phys. C **40**, 100001 (2016) and 2017 update.
[2] C. Picciotto, Phys. Rev. D **45**, 1569 (1992).
[3] L. W. Bartel *et al.* (JADE Collaboration), Phys. Lett. B **113**, 190 (1982).
[4] H. Behrends *et al.* (CELLO Collaboration), Phys. Lett. B **114**, 378 (1982); Phys. Lett. B **125**, 518E (1983).
[5] C. Berger *et al.* (PLUTO Collaboration), Phys. Lett. B **142**, 125 (1984).
[6] M. Althoff *et al.* (TASSO Collaboration), Phys. Lett. B **147**, 487 (1984).
[7] H. Aihara *et al.* (TPC/$\gamma\gamma$ Collaboration), Phys. Rev. D **35**, 2650 (1987).
[8] H. Albrecht *et al.* (ARGUS Collaboration), Phys. Lett. B **199**, 457 (1987).
[9] S. Bityukov *et al.*, Z. Phys. C **50**, 451 (1991).
[10] J. Wess and B. Zumino, Phys. Lett. B **37**, 95 (1971); E. Witten, Nucl. Phys. B**223**, 422 (1983).
[11] M. Benayoun *et al.*, Z. Phys. C **58**, 31 (1993); M. Benayoun, P. David, L. DelBuono, O. Leitner, Eur. Phys. J. C **65**, 211 (2010);
[12] A. Abele *et al.* (Crystal Barrel Collaboration), Phys. Lett. B **402**, 195 (1997).
[13] M. Acciarri *et al.* (L3 Collaboration), Phys. Lett. B **418**, 399 (1998).
[14] F. Stollenwerk *et al.*, Phys. Lett. B **707**, 184 (2012).
[15] F. Jegerlehner and A. Nyffeler, Phys. Rep. **477**, 1 (2009).
[16] C. Hanhart *et al.*, Eur. Phys. J. C **73**, 2668 (2013); Erratum: [Eur. Phys. J. C **75**, 242 (2015)].
[17] P. Adlarson *et al.* (WASA-at-COSY Collaboration), Phys. Lett. B **707**, 243 (2012).
[18] D. Babusci *et al.* (KLOE Collaboration), Phys. Lett. B **718**, 910 (2013).
[19] M. Ablikim *et al.* (BESIII Collaboration), Chin. Phys. C **41**, 013001 (2017).
[20] M. Ablikim *et al.* (BESIII Collaboration), Nucl. Instrum. Methods Phys. Res., Sect. A **614**, 345 (2010).
[21] M. Ablikim *et al.* (BESIII Collaboration), Phys. Rev. Lett. **118**, 012001 (2017).
[22] J. C. Chen, G. S. Huang, X. R. Qi, D. H. Zhang, Y. S. Zhu, Phys. Rev. D **62**, 034003 (2000).
[23] D. J. Lange, Nucl. Instrum. Methods Phys. Res., Sect. A **462**, 152 (2001); R.-G. Ping, Chin. Phys. C **32**, 599 (2008).
[24] R. R. Akhmetshin *et al.*, Phys. Lett. B **527**, 161 (2002).
[25] G. J. Gounaris, J. J. Sakurai, Phys. Rev. Lett. **21**, 244 (1968).
[26] J. P. Lees *et al.* (BABAR Collaboration), Phys. Rev. D **86**, 032013 (2012).
[27] M. Ablikim *et al.* (BESIII Collaboration), Phys. Lett. B **753**, 629 (2016).
[28] R. R. Akhmetshin *et al.* (CMD-2 Collaboration), Pisma Zh. Eksp. Teor. Fiz. **84**, 491 (2006)[JETP Lett. **84**, 413 (2006)]; R. R. Akhmetshin *et al.* (CMD-2 Collaboration), Phys. Lett. B **648**, 28 (2007); A. Aloisio *et al.* (KLOE Collaboration), Phys. Lett. B **606**, 12 (2005).
[29] B. Aubert *et al.* (BABAR Collaboration), Phys. Rev. Lett. **103**, 231801 (2009).
[30] F. Ambrosio *et al.* (KLOE Collaboration), Phys. Lett. B **700**, 102 (2011).
[31] S. R. Amendolia *et al.* (NA7 Collaboration), Nucl. Phys. B**277**, 168 (1986).
[32] B. Kubis and J. Plenter, Eur. Phys. J. C **75**, 283 (2015).
[33] See Supplemental Material at http://link.aps.org/supplemental/10.1103/PhysRevLett.120.242003 for the summary of systematic uncertainties on the model-dependent fits and on the model-independent fit.
[34] M. Ablikim *et al.* (BESIII Collaboration), Phys. Rev. D **87**, 012002 (2013).
[35] M. Ablikim *et al.* (BESIII Collaboration), Phys. Rev. D **81**, 052005 (2010).
[36] C. Hanhart, S. Holz, B. Kubis, A. Kupsc, A. Wirzba, C. W. Xiao, Eur. Phys. J. C **77**, 98 (2017).